Basic research and application of anodic oxide films on aluminum

-Barrier type and Porous type-

H. Takahashi
Nippon Chemi-Con Co.
(Professor Emeritus of Hokkaido Univ.)

Kinki Aluminum Finishing Research Soc.
Hotel Awina Osaka
April. 24, 2015

Oxide and Hydroxide Films on Aluminum

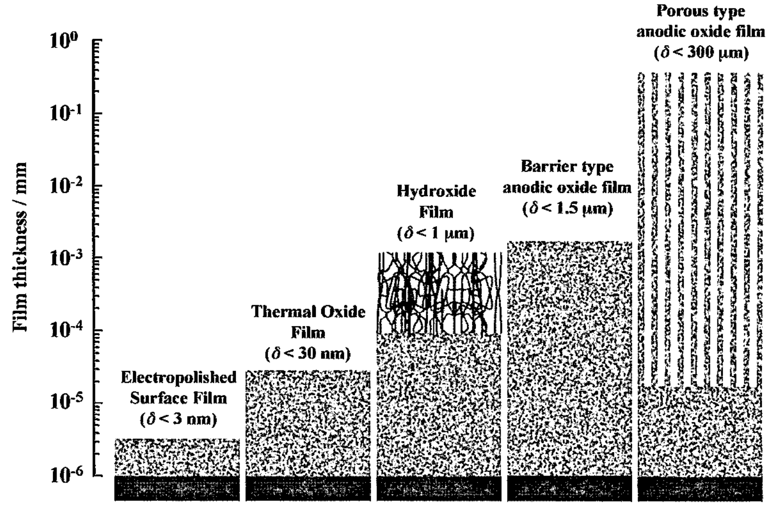

Anodizing (Oxide film formation by anodic oxidation)

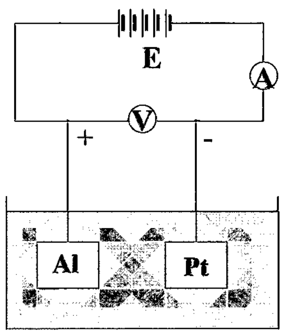

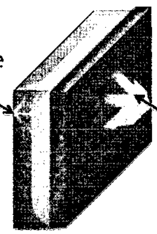

Barrier type and porous type anodic oxide films

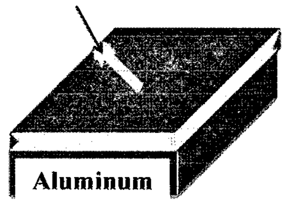

Barrier type

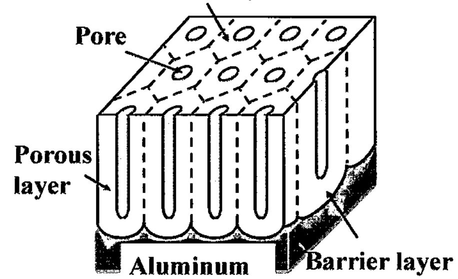

Porous type

近畿アルミニウム表面処理研究会・春季特別講演会 2015

High field theory on oxide film formation

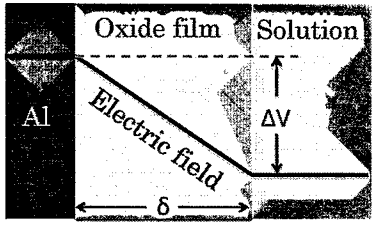

$I = A \exp(BE)$

$= i_0 \exp(B\, \Delta V/\delta)$

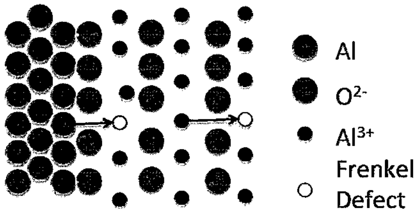

A. Guntherschultz, H. Betz: Z. Phys. 71 (1931)

J. W. Verwey: Physica, 2, 1059 (1935)

N. Cabrera, N. F. Mott: Rep. Prog. Phys., 12, 163 (1948)

J. F. Dewald, Acta Metall: 2, 340 (1954).

Ion transport during anodizing

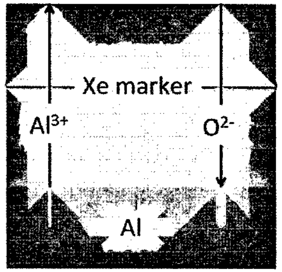

Transport of Al^{3+} and O^{2-} ions

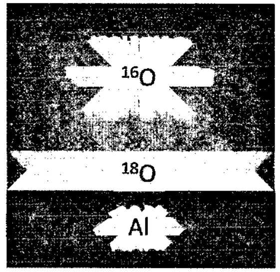

Order remaining of ^{16}O and ^{18}O

J.A. Davies, B. Domeiji, J.P.S. Prongle and F. Brown: J. Electrochem. Soc. 112, 675 (1965)
J.P.S. Pringle: J. Electrochem. Soc. 120, 1391 (1973)

Electron beam-induced-crystallization

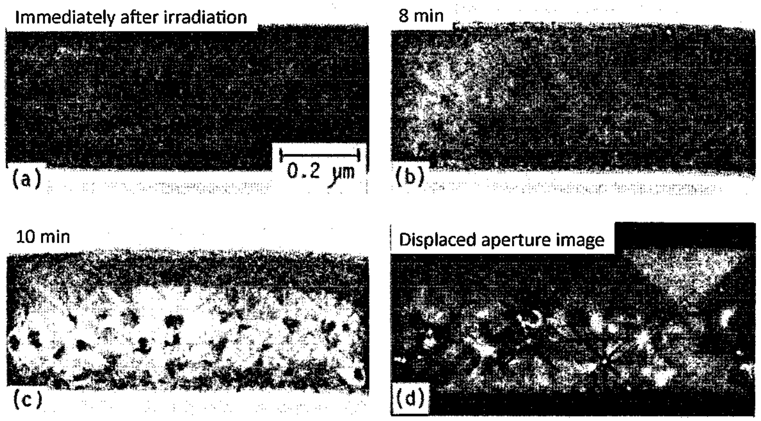

K. Shimizu, G. E. Thompson, and G. C. wood, Thin solid Films, 77, 318 (1981)

Effects of transport of electrolytic anions on the structure of anodic oxide films

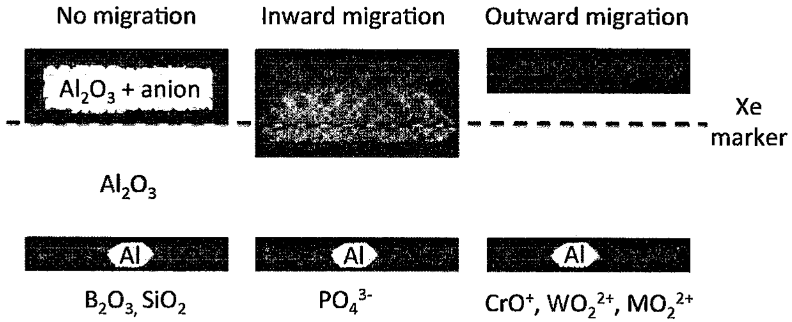

Chemical Bond energy between Me^{n+} and O^{2-}

H. Habazaki, K. Shimizu, P. Skeldon, G. e. Thompson, G. C. Wood, J. Surf. Sci. Soc. Jpn., 19, 772 (1998)

Anodizing of dilute, metastable binary aluminum alloys

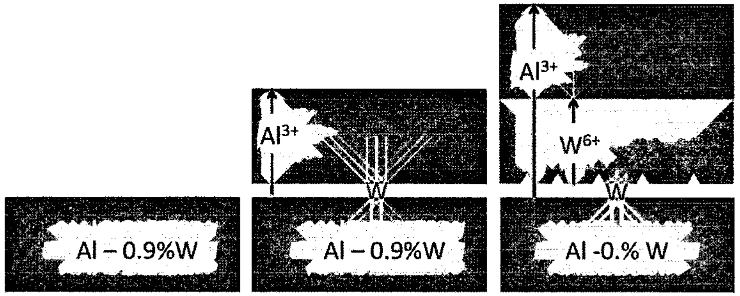

Enrichment of W at the interphase
before incorporation into the oxide film

H. Habazaki, K. Shimizu, T, P. Skeldon, G. E. Thompson, G. C. Wood and X. Zhou: Corros. Sci., 39, 731 (1997)

Relationship between Enrichment of alloying elements and ΔG for the oxide formation

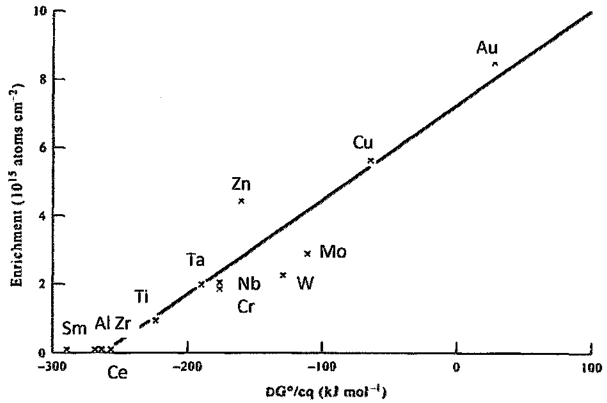

H. Habazaki, K. Shimizu, T, P. Skeldon, G. E. Thompson, G. C. Wood and X. Zhou: Corros. Sci., 39, 731 (1997)

Application of barrier oxide films

-Al electrolytic capacitor-

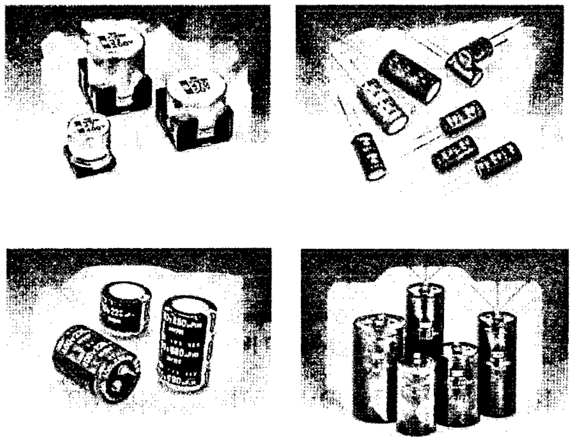

Formation of crystalline oxide film by anodizing after hydrothermal treatment

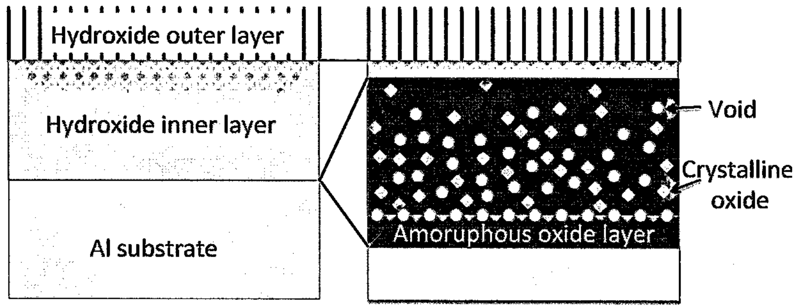

After hydrothermal treatment　　After anodizing

H. Tkahashi, Y. Umehara, H. Miyamoto, N. Fujimoto, and M. Nagayama, J. Surf. Fin. Soc. Jpn., 38, 67, 138 (1985)

Formation of Crystalline oxide film by anodizing after thermal treatment

Thermal oxide film (γ-Al_2O_3)

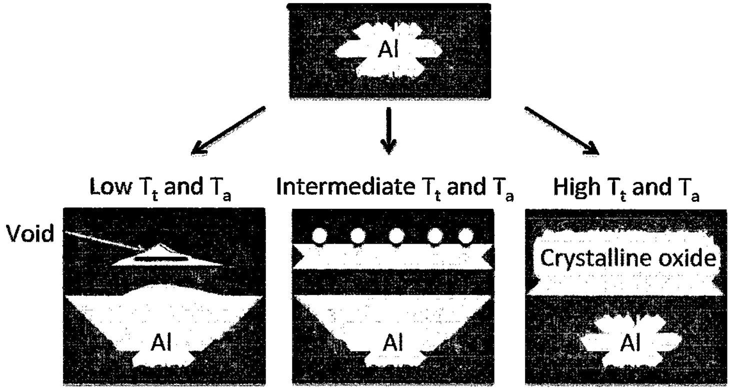

Shimizu et al. (1985) Crevecoeur et al.(1987) H. Takahashi et al. (1991)

Ta-Al Composite Oxide Films Formed in a Tunnel Etched Pore by MOCVD/Anodizing

MOCVD(723 K) + Anodizing up t o100 V

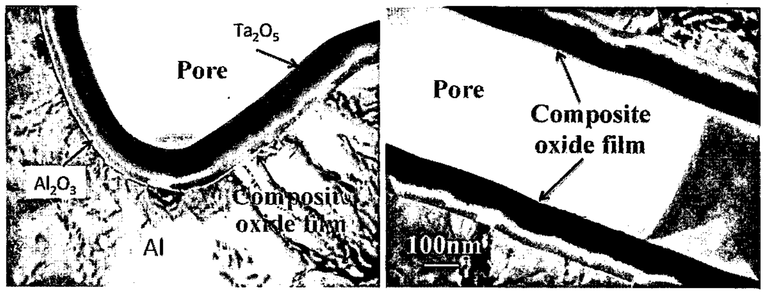

Capacitances of Ta-Al composite oxide films are much higher than that of Al_2O_3 films formed by anodizing.

100 V: 100 %, 200 V: 75 %, 300 V: 20 % higher

TEM images of electropolished specimens anodized up to E_a = 200, 400, 600, 800, and 1000V after sol-gel dip coating of SiO_2 (n = 4)

Element \ Position	1	2	3	4	5
Si	15.7	13.5	10.4	8.9	0.0
O	66.7	65.4	68.0	63.6	63.1
Al	17.6	21.1	21.6	27.5	36.9

EDX analysis (at%)

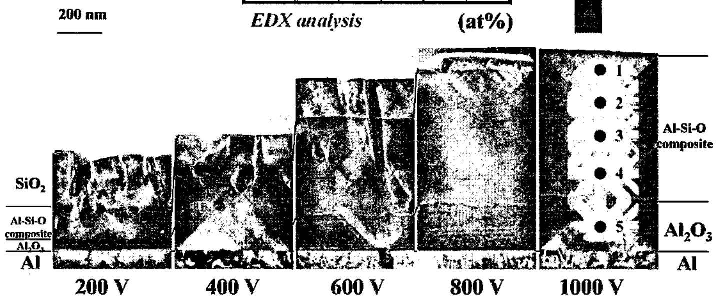

K. Watanabe, M, Sakairi, H. Takahashi, K. Takahiro, S. Nagata, and S. Hirai
J. Electrochem. Soc., **148**, B473 (2001)

Structural Features of Oxide Coatings on Aluminum

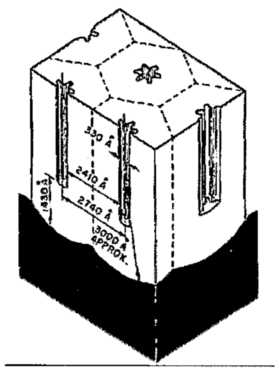

Electron microscopy

H_2SO_4, $H_2C_2O_4$, H_3PO_4, H_2CrO_4

Hexagonal cellular structure

Cell size and barrier layer thickness depends on forming voltage

F. Keller, M. S. Hunter, and D. L. Robinson,
J. Electrochem. Soc., 100, 411 (1953)

Dissolution mechanism during open circuit

Pore widening

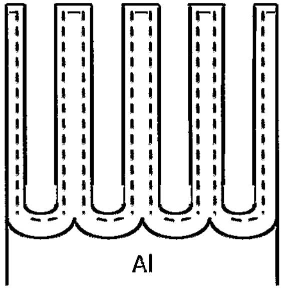

Pore shortening

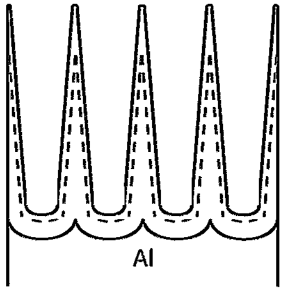

M. Nagayama, K. Tamura, and H. Takahashi
Corros. Sci., **12**, 133-136 (1972)

J. W. Diggle, T. C. Downie and C. W. Goulding,
J. Electrochem. Soc, 116, 1347 (1969)

Dissolution mechanism of pore-sealed oxide film

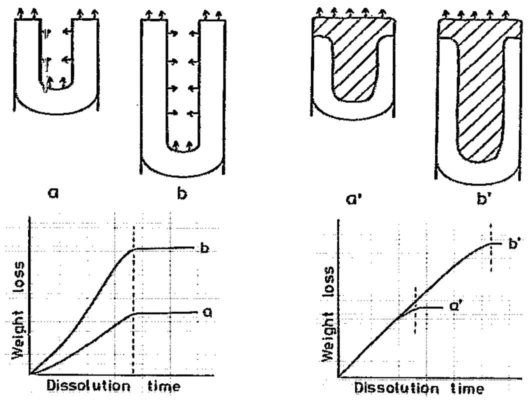

M. Koda, H. Takahashi, and M. Nagayama, Surf. Fin. Soc. Jpn., 33, 242 (1982)

Chemical structure of porous anodic oxide films.

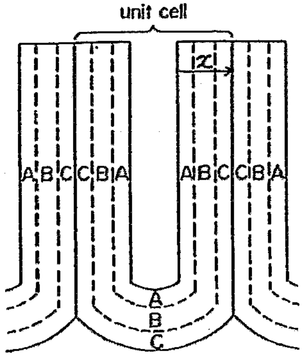

A. $Al_{2-x}H_{3x}O_{3-y}\,(Anion^{p-})_{2y/p}$
B. $Al_2O_{3-y}\,(Anion^{p-})_{2y/p}$
C. Al_2O_3

H. Takahashi and M. Nagayama, J. Chem. Soc. Jpn., 1974, 453 (1974)
Thompson, G. E.; Furneaux, R. C.; Wood, G. C. Corros. Sci., 18, 481 (1978)
Y. Fukuda and T. Fukushima, Bull.Chem. Soc. Jpn, 53, 3125 (1980)
Ono, S.; Masuko, N. Corros. Sci., 33, 503 (1992)

Changes in cell size, 2R, pore-diameter, 2r, and number of pores, N, with anode potential

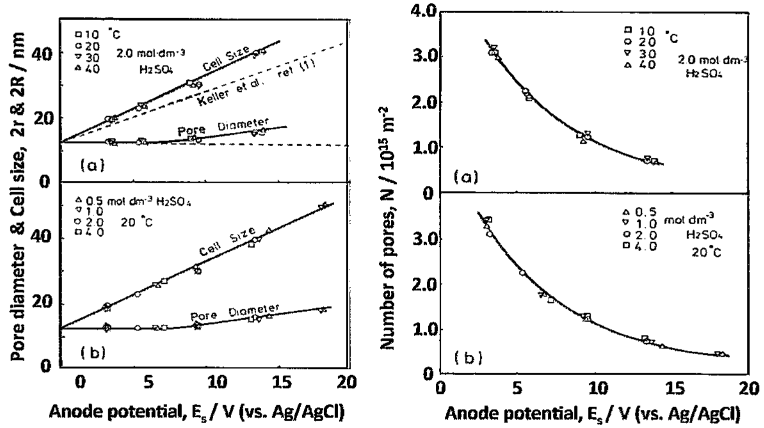

K. Ebihara, H. Takahashi, and M Nagayama, J. Surf. Fin, Soc.Jpn., 35, 205 (1984)

Pore initiation mechanism

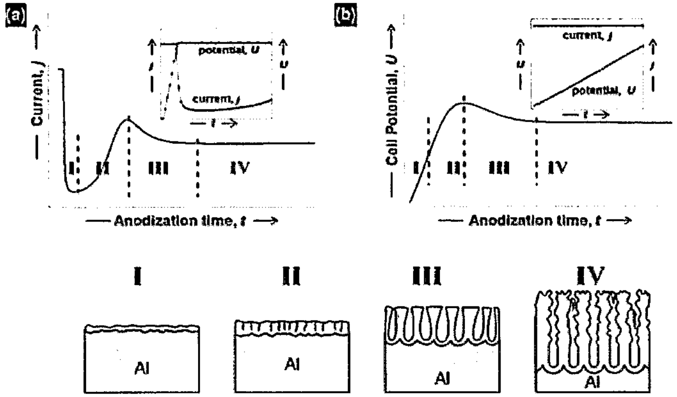

W. Lee and Sang-J. Park: Chem Rev. 114, 7487 (2014)

Film growth at steady state

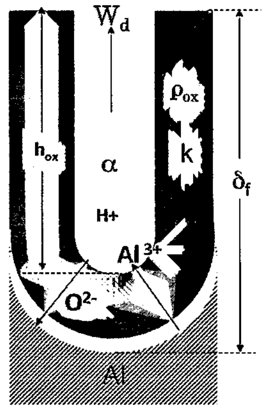

T_{Al}: Transport number of Al^{3+} ions

Volume of oxidized Al: $V_{T(Al)}$

$V_{T(Al)} = W_{T(Al)} / \rho_{Al}$ (1)

$W_{T(Al)}$: amount of oxidized Al

ρ_{Al} : density of Al

Total Volume of formed oxide: $V_{T(ox)}$

$V_{T(ox)} = V_{ox} + V_p = W_{T(ox)} / \rho_{ox}$

$= W_{T(Al)} (1 - T_{Al}) / (k \rho_{ox})$ (2)

V_{ox} : volume of oxide film

V_p : volume of pore

$W_{T(ox)}$: Total amount of formed oxide

ρ_{ox} :density of oxide film

K: mass ratio of Al in oxide film

Pilling-Bedworth ratio:

$R_{P.B.} = V_{T(ox)} / V_{T(Al)} = (1 - T_{Al}) / (k \rho_{ox} / \rho_{Al})$

Volume expansion of specimen by the formation of porous type anodic oxide films

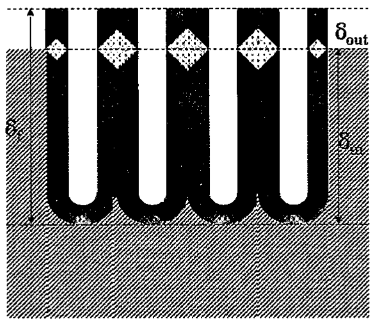

$(\delta_{out} + \delta_{in}) / \delta_{in}$

$= 1.35 - 1.65$

Vrublevsky I., Parkuon V. Schreckenbach, and J. Marx G. Appl. Surf. Sci., 220, 51(2003)

SEM image of the vertical cross section of the aluminum specimen after anodizing

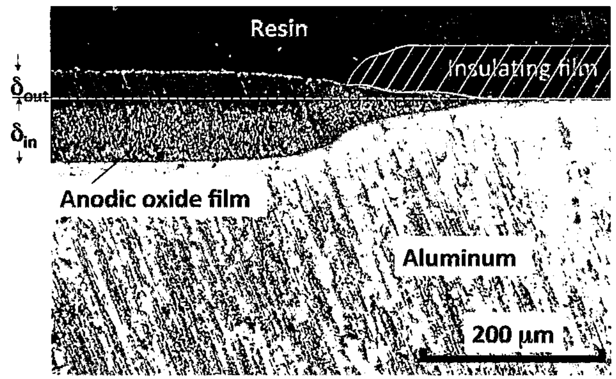

0.22 kmol m^{-3} oxalic acid at T = 293 K with 150 Am^{-2} for 4h

H. Takahashi et al., Modern Aspects of Electrochemistry 46, p.91 (2009)

TEM images of vertical sections of anodic oxide film formed on Al-3.5%W in phosphoric acid solution

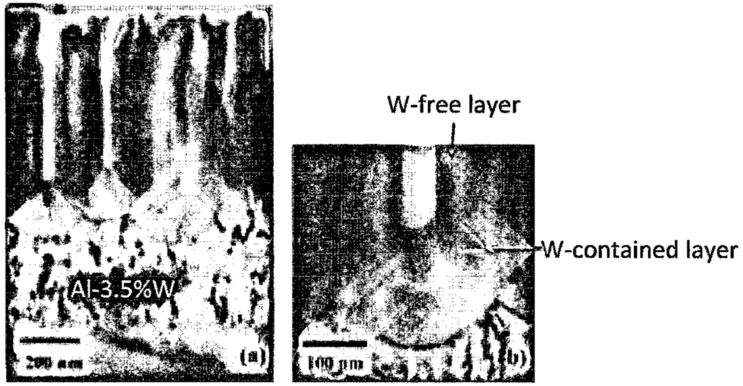

S. J. Garcia-Vergara, P. Skeldon, G. E. Thompson, T. Hashimoto, and H. Habazaki, J. Electrochem. Soc., 154, C540 (2007)

W tracer movement in oxide films during anodizing of Al-W alloy sputtered Al in phosphoric acid solution

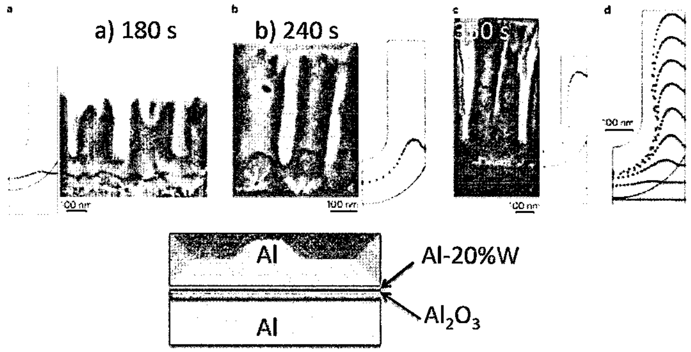

F. Zhou, D. J. LeClere, S. J. Garcia-Vergara, T. Hashimoto, S. Molchan, H. Habazaki, P. Skeldon, and G. E. Thompson, J. Electrochem. Soc., 157, C437 (2010)

Velocity vectors and mean stress in barrier layer during anodizing

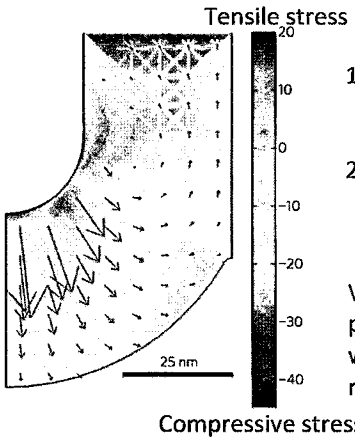

1. High compressive-stress at pore base regions
2. Low compressive-stress at oxide/metal interface region

Viscous flow of film material from pore base region toward the cell walls and upper flow at the cell wall regions

J. E. Houser and K. R. Hebert, Nature Materials, 8, 415 (2009)

Electrolytic coloring of anodized aluminum

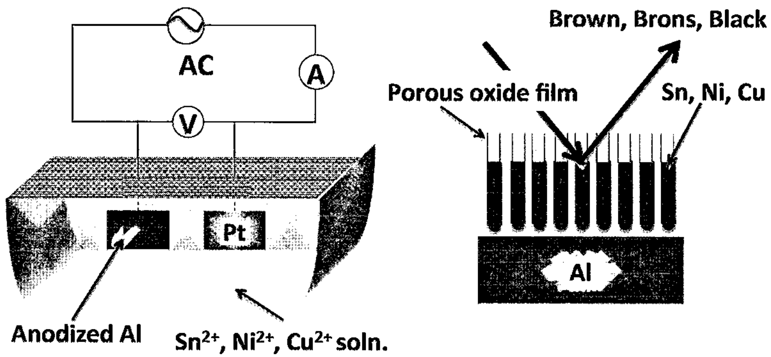

T. Asada, US 4022671 A (1977)

近畿アルミニウム表面処理研究会・春季特別講演会 2015

Fabrication of highly ordered cell structure (1)

1. Anodizing with long period
Self arrangement of cell structure by long anodizing

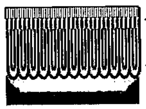

2. Double step anodizing
Texturing of the surface by film dissolution

H. Masuda and K. Fukuda Sci.,268, 1466 (1995)

Fabrication of highly ordered cell structure (2)

3. Mold texturing

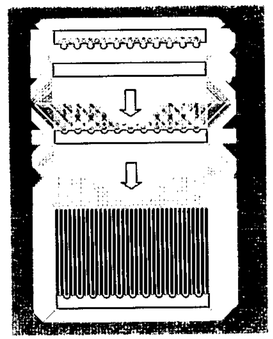

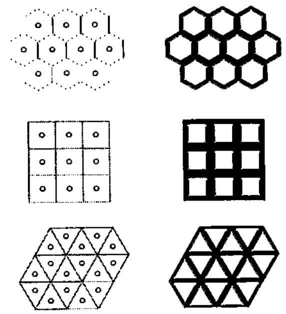

H. Masuda, H. Yamada, M. Satoh, H. Asoh, M. Nakao and T. Tamamura, Appl. Phys. Lett., 71, 2770 (1997)

SEM images of ideally ordered anodic porous oxide alumina by pre-texturing with mold

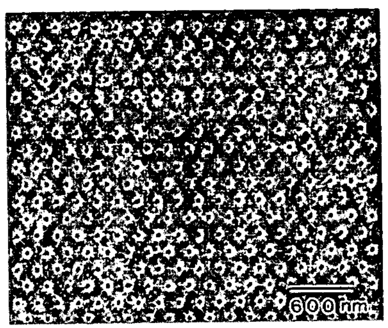

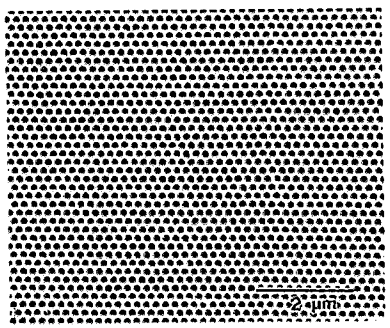

H. Asoh, K. Nishio, M. Nakao, T. Tamamura, H. Masuda, J. Electrochem. Soc., 148, B152 (2001)

Template Synthesis of Metal Microtubules

Au sputtering ➡ Au electroplating ➡ Oxide film dissolution

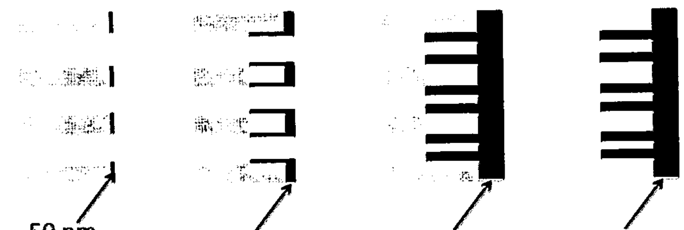

C. J. Brumlik & C. R. Martin J. Am. Chem. Soc., 113, 3174 (1991)

Formation of nano-rod and nano-tube by filling-up into pores of porous anodic oxide films

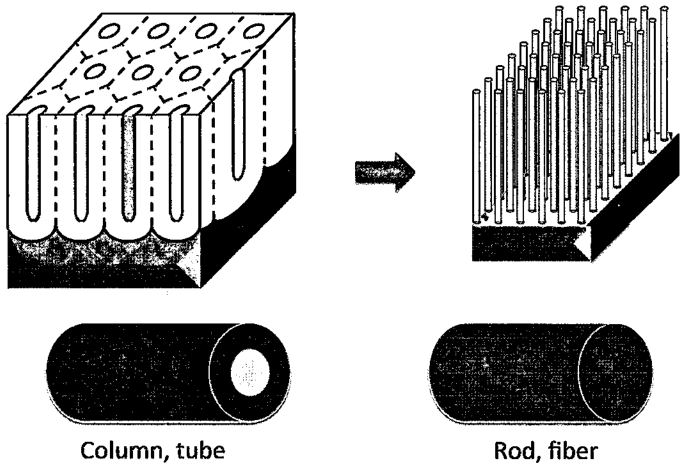

Principles of laser irradiation/anodizing processing

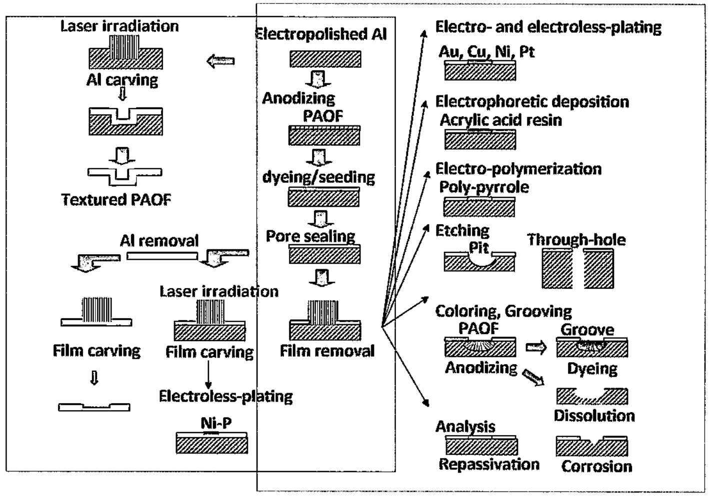

H. Takahashi et al., Modern Aspects of Electrochemistry 46, p.91 (2009)

Laser Irradiation setup

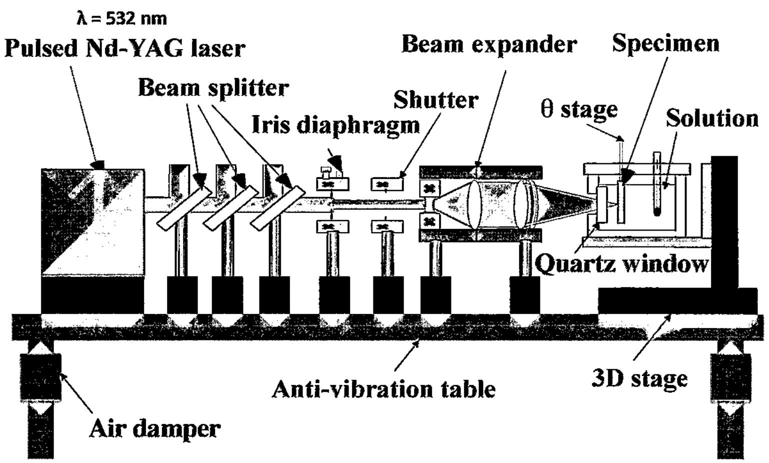

Applications of Laser Irradiation Technique

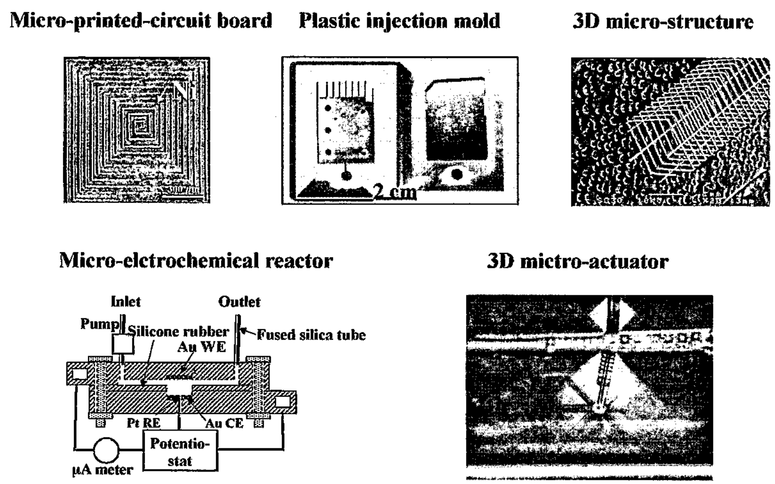

Procedure of Fabrication of 3D manipulator

Electropolished cylindrical Al tube
(99.50 %, outer diameter= 2 mm, inner diameter= 1.6 mm)

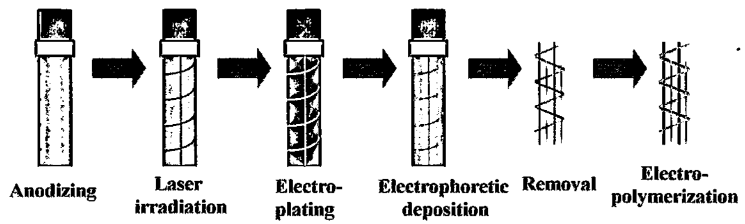

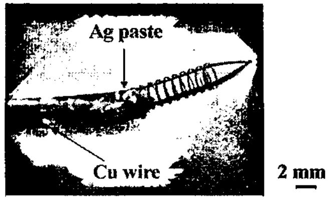

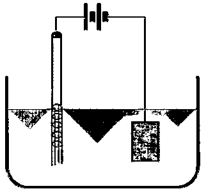

Electropolymerization

3D manipulator

Mulite cylinder
($3Al_2O_3 \cdot 2SiO_2$)
Outer diameter : 1.5 mm
Inner diameter : 0.5 mm
Length : 2.1 mm
V : 3.2 mm^3
W : 6.5 mg

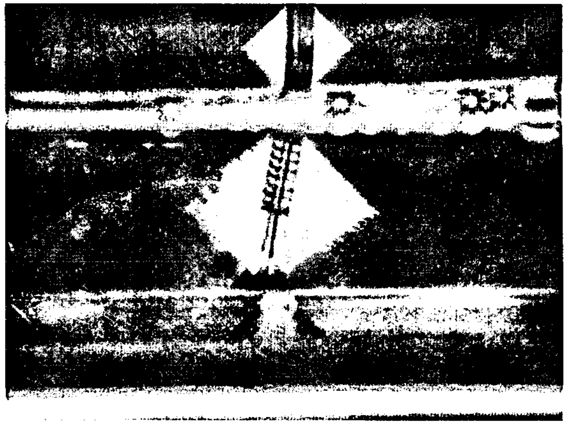

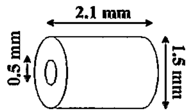

Application of AFM Probe Processing

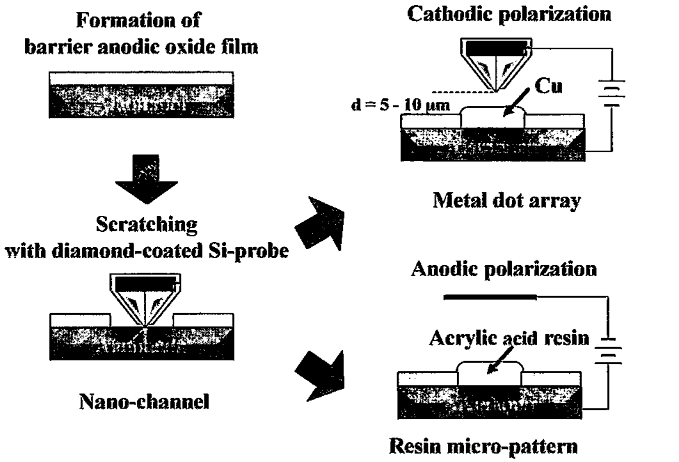

Z. Kato, M. Sakairi, and H. Takahashi: Zairyo-to-kankyo, **52**, 12 (2003)
S. Kurokawa, T. Kikuchi, M. Sakairi, and H. Takahashi, Electrochim. Acta, **53**, 8118 (2008)

Micro- and nano-patterns by AFM processing